Journal of Catalysis 266 (2009) 291–298

Contents lists available at ScienceDirect

Journal of Catalysis

journal homepage: www.elsevier.com/locate/jcat

Effects of individual promoters on the Direct Synthesis of methylchlorosilanes

Alexander D. Gordon [a], B.J. Hinch [b], Daniel R. Strongin [a,*]

[a] Department of Chemistry, Temple University, Philadelphia, PA 19122, United States
[b] Department of Chemistry and Chemical Biology, Rutgers University, Piscataway, NJ 08854, United States

ARTICLE INFO

Article history:
Received 8 May 2009
Revised 22 June 2009
Accepted 23 June 2009
Available online 3 August 2009

Keywords:
Methylchlorosilane
Dimethyldichlorosilane
Dichloromethylsilane
Trichloromethylsilane
Attenuated total reflection
Fourier transform infrared spectroscopy

ABSTRACT

The industrially relevant Direct Synthesis involves the reaction of methyl chloride with silicon in the presence of a copper catalyst (promoted with Zn, Sn, and P), termed the contact mass, to form methylchlorosilanes. *In situ* attenuated total reflection Fourier transform infrared spectroscopy (ATR-FTIR) coupled with flow reactor studies was used to help understand the relationship between the composition of the working catalytic surface and product selectivity during reaction (1 bar CH_3Cl at 300 °C). Promotion of copper–silicon contact masses with Sn and Zn increased the selectivity of the reaction for dimethyldichlorosilane compared to P-promoted and copper–silicon (unpromoted) contact masses. Results showed that the rate of Si conversion associated with the Sn-promoted contact mass was higher than the Si conversion rate associated with the Zn and unpromoted contact masses. ATR-FTIR results suggested that Sn promotion led to a stabilization and relatively high concentration of surface methyl species. In contrast to Sn or Zn promotion, P promotion led to significant methyl fragmentation on the contact mass surface, consistent with its relatively low selectivity toward dimethyldichlorosilane.

1. Introduction

The Direct Synthesis (DS) of methylchlorosilanes from the reaction of methyl chloride (MeCl), CH_3Cl, with silicon, also known as the Rochow Synthesis, was developed by Eugene Rochow for the efficient production of methylchlorosilane monomers for the silicone industry [1]. The most desirable of these monomers to date has been dimethyldichlorosilane (DMDCS), but it is possible that future applications may require different monomeric precursors. The contact mass associated with the DS is comprised of silicon with 1–10% (by weight) copper that constitutes the catalytic component. The unpromoted contact mass, however, is relatively unselective for the synthesis of DMDCS until parts-per-million amounts of promoters, such as Sn, Zn, and P are added to the unpromoted contact mass. These additives are termed promoters, since they increase the reactivity and selectivity of the unpromoted contact mass toward the desired methylchlorosilanes. The DS reaction can be represented by the following reaction:

$$MeCl_{(g)} + Si_{(s)} \xrightarrow{\text{Cu catalyst, Promoters (300 °C)}} Me_xSiH_yCl_{z(g)}$$

where $x + y + z = 4$

Due to the importance of the DS, the mechanistic details that contribute to product formation have been studied for decades. Excellent reviews have summarized much of the understanding that has resulted from prior studies [2–5]. While the mechanistic detail by which the promoters act is still lacking, there are general statements that can be made concerning the effects of promoters, such as Zn, Sn, and P, on the reactivity and selectivity of the unpromoted contact mass. Prior research, for example, has shown that a copper–silicon contact mass promoted with only Zn leads to an increased selectivity for DMDCS although it typically does not have a significant effect on the rate [6,7]. In contrast, contact masses promoted with only Sn exhibit an enhanced rate compared to Zn and a higher selectivity toward DMDCS. It has been postulated in prior studies that zinc increases silicon diffusion to sites above a threefold copper site [8]. Phosphorus (typically added as copper phosphide) was introduced as a promoter for the DS in 1990 by the Dow Corning Corporation. The addition of copper phosphide to the contact mass (with Zn and or Sn) increases the selectivity for DMDCS [9]. It has been postulated that copper phosphide promotes active phase formation. No published studies exist, however, which have investigated the effect of phosphorus when it is the only promoter present in a contact mass.

Prior studies that have investigated the action of promoters [3] on the DS have utilized a range of experimental techniques that have included temperature programmed desorption [10], scanning electron microscopy [8,11], scanning Auger electron microscopy [12,13], X-ray diffraction [12], and X-ray photoelectron spectroscopy [12]. These previous studies have largely studied the influence of promoters on silicon diffusion processes and have not generally addressed the effect of the promoters on the dissociative chemisorption of MeCl and the resulting generation of methyl and chlorine surface groups. Furthermore, these prior studies have

* Corresponding author.
E-mail addresses: Alex.Gordon@temple.edu (A.D. Gordon), jhinch@rutchem.rutgers.edu (B.J. Hinch), dstrongi@temple.edu (D.R. Strongin).

0021-9517/$ - see front matter © 2009 Elsevier Inc. All rights reserved.
doi:10.1016/j.jcat.2009.06.026

largely consisted of *ex situ* studies that have investigated the composition of the DS contact mass after reaction. Hence, information that is concerned with the composition of the surface monolayer associated with the working DS contact mass is not yet available.

In contrast to prior studies, research presented in this contribution investigates the chemical structure of the working catalytic surface *in situ* under real conditions. Attenuated total reflection Fourier transform infrared spectroscopy (ATR-FTIR) was used to investigate the structure of the working contact masses as a function of promoter and reaction time. This information on the structure of the surface monolayer was combined with studies of the temporal behavior of the product selectivity as a function of promoter. Relationships between the structure of the surface monolayer under working conditions and product selectivity were developed that help to elucidate the promoter action. To the best of our knowledge, this is the first study to investigate the DS *in situ* with an emphasis on understanding the effect of promoters on the surface concentration and reactions of surface intermediates.

2. Materials and methods

Silicon, copper, tin, and zinc used to make the various contact masses in this study were purchased from commercial suppliers. Silicon (98.5%), zinc (⩾99%, powder), and tin (⩾99%) were obtained from Aldrich and copper (in the form of CuCl, ⩾99%) was obtained from Sigma–Aldrich. CuP (99.999%) was obtained from American Elements. The percentage weight compositions of the Cu and promoters associated with the contact masses used in this study were typical of those described in the literature [3,4] and consisted of the following: (1) unpromoted, 10% Cu; (2) zinc promoted, 10% Cu and 0.06% Zn; (3) phosphide promoted, 10% Cu and 0.02% P (added as CuP); (4) tin promoted, 10% Cu and 0.004% Sn. Each contact mass formulation was stored as a slurry in hexane.

Individual contact masses with and without promoter (~50 mg) were added as a slurry on to a diamond ATR lens that was integrated into an ATR-FTIR reaction cell (Specac Supercritical GoldenGate ATR™ and Thermo Electron Magna 560). This cell was in line with a fixed bed stainless steel reactor that contained 1.5 g of the same contact mass that was present in the ATR reaction cell. The ATR-FTIR cell and reactor were individually resistively heated to 300 °C. The cell and reactor were set up in series using Teflon (DuPont™) tubing. A schematic of the experimental setup is shown in Fig. 1. Control experiments were performed to verify that the small amount of product that presumably formed in the gas stream from the 50 mg of contact mass in the ATR reactor had no observable influence on the product distribution, silicon conversion, and MeCl conversion derived from the effluent of the fixed reactor bed. A sampling valve (Valco) was present at the exit of the flow reactor and aliquots of the effluent were bypassed into a gas chromatograph (GC) at specified times for product analysis. The GC (HP 5890) was equipped with a 15 m silica column and a thermal conductivity detector. The sensitivity of the thermal conductivity detector for the different products analyzed in this contribution was determined by passing known amounts of pure samples through the GC and measuring the detector response.

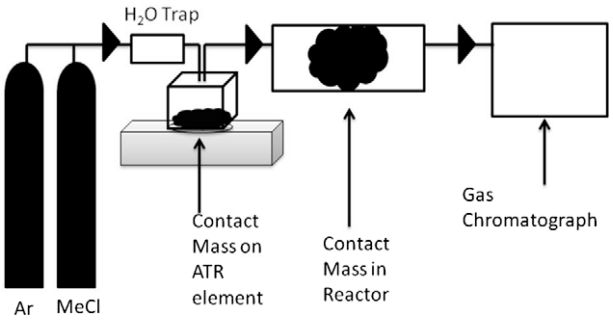

Fig. 1. A schematic of the experimental setup used in this study. MeCl was first flowed over 25 mg of contact mass on a diamond ATR element. The MeCl reactant was then passed through a flow reactor containing 1.5 g of contact mass. The production of methylchlorosilanes was determined by passing samples of the effluent through a gas chromatograph.

A typical experimental run consisted of flowing argon (99.997%, Air Products) at a rate of 0.1 standard cubic feet/h continuously over the contact mass mixture until both the reactor and cell were at 300 °C. A moisture trap (Vici Moisture Trap, model T100-2) was placed inline to minimize contaminant in the gas stream. No oxygen scrubber was used in this setup. The Ar was kept flowing for an additional period of 1 h at 300 °C. $SiCl_4$ product was detected after the contact mass reached 300 °C, but this product decreased in yield over time and by 2–3 h it was no longer detectable. We suspect that this product was the result of chlorine release during the alloying process between the Si and Cu (initially present as CuCl). At this point an infrared spectrum was obtained and then the Ar was replaced by MeCl (99.99%, Matheson Tri Gas). The infrared spectrum taken in the Ar flow served as the reference for subsequent data taken in the presence of MeCl. GC analysis of the effluent from the reactor and infrared data were acquired every 15 min during the DS reaction. Experimental runs reported in this contribution lasted for times up to 6 h.

MeCl conversions (in %) quoted in this contribution were calculated on the basis of Eq. (1) while selectivity and −Δmass/h (referred to as Si conversion) quantities were calculated on the basis of Eqs. (2) and (3), respectively. GC peak areas were determined using Peak Simple software (SRI Instruments):

$$\text{MeCl conversion } (\%) = \frac{\text{moles silane}}{\text{moles MeCl} + \text{moles silane}} \times 100 \quad (1)$$

$$\text{Selectivity } (\%) = \frac{\text{moles silane}}{\sum \text{moles silane products}} \times 100 \quad (2)$$

$$-\Delta\text{mass } (\%)/\text{h} = \frac{\text{final moles Si} - \text{initial moles Si}}{\text{initial moles Si} \times \text{reaction time}} \times 100 \quad (3)$$

3. Results and discussion

3.1. Promoter effects on selectivity, MeCl conversion, and Si conversion

Fig. 2 displays the selectivity for DMDCS, dichloromethylsilane (DCMS), and trichloromethylsilane (TCMS) as a function of exposure time to MeCl at 300 °C for the unpromoted, P-promoted, Zn-promoted, and Sn-promoted contact masses. Other products observed included dimethylchlorosilane and trimethylchlorosilane but the data for these products are not presented in this contribution. The contact mass with the highest selectivity toward DMDCS (Fig. 2, *top*) contained Sn promoter (72%). The maximum selectivity for this specific product associated with the Zn-promoted, P-promoted, and unpromoted contact masses was 53%, 17%, and 31%, respectively. Experimental runs were limited to 6 h.

While the selectivity of the P-promoted contact mass was exceedingly low toward DMDCS, it exhibited the highest selectivity (65%) of the four different contact masses toward DCMS (Fig. 2, *middle*). Interestingly, the initial selectivity of the unpromoted catalyst for this product was ~0% after 0.5 h, but it rose to a value of 28% after 5 h. The other three contact masses showed less significant changes in their selectivity toward this product over the 6 h time period. Finally, Fig. 2 (*bottom*) displays TCMS selectivity for the different contact masses. For this product, the unpromoted

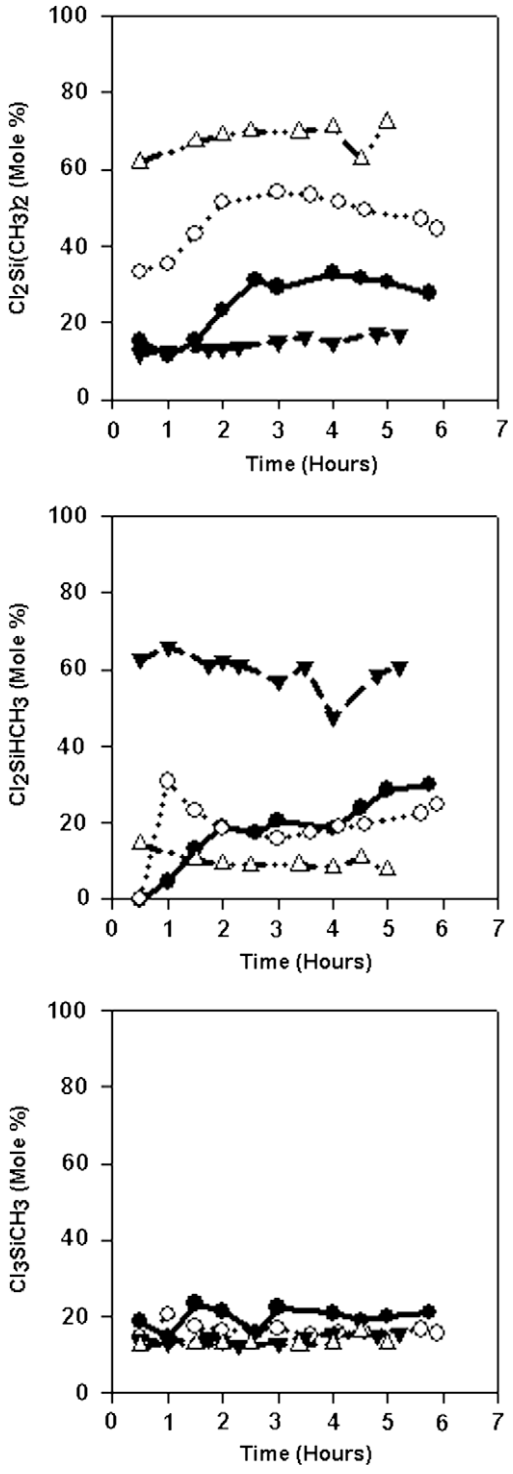

Fig. 2. The selectivities for DMDCS [$Cl_2Si(CH_3)_2$] (*top*), DCMS [Cl_2SiHCH_3] (*middle*), and TCMS [Cl_3SiCH_3] (*bottom*) are plotted as a function of time for the unpromoted (●), P-promoted (▼), Sn-promoted (△), and Zn-promoted (○) contact masses.

contact mass showed the highest selectivity, while the P- and Sn-promoted contact masses exhibited the lowest selectivities (~13%).

Fig. 3 displays MeCl conversion as a function of reaction time for the different contact masses. Initially, the Sn- and P-promoted catalysts each showed a MeCl conversion of ~5%. However, the Sn-promoted system exhibited a significant increase in MeCl conversion as the DS reaction proceeded over the 5 h reaction time. At 5 h, the Sn-promoted catalyst reached a MeCl conversion of 30%,

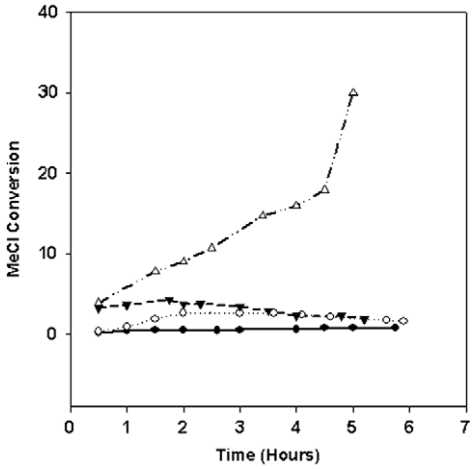

Fig. 3. MeCl conversion is plotted as a function of time for unpromoted (•), P-promoted (▼), Zn-promoted (○), and Sn-promoted (△) contact masses. The unpromoted contact mass demonstrates very low MeCl conversion throughout the run. The P-promoted contact mass has high MeCl conversion earlier in the run, but decreases after two hours. The Zn-promoted contact mass shows a longer induction period than the other promoted contact masses, requiring 3 h to reach maximum MeCl conversion. The Sn-promoted contact mass shows greater MeCl conversion than the other contact masses.

which was a factor of 7 higher than any of the other catalyst formulations. Both the P-promoted and Zn-promoted formulations exhibited MeCl conversions that never rose above 5% within the first 2 h. After this time, both of these systems exhibited a small drop in the amount of MeCl conversion; albeit the decrease was only 2–3%. The unpromoted catalyst showed the poorest MeCl conversion, never exceeding 2–3%.

Fig. 4 exhibits the $-\Delta$mass/h that is based on the weight difference of the different contact masses before and after a 6 h exposure to MeCl. It is assumed that this measure is primarily due to the rate of Si conversion to gaseous product, but the addition of carbon and chlorine species that are inactive on the surface likely has an effect on the mass change of the contact mass. Examination of these data

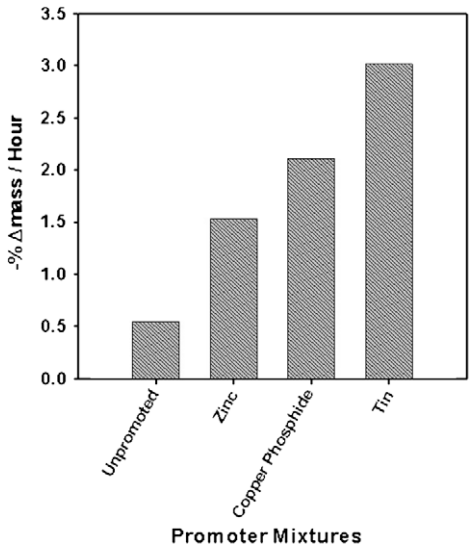

Fig. 4. The relative percentage change in mass per hour is shown for the unpromoted, Zn-promoted, P-promoted, and Sn-promoted contact masses. Note that since overall mass is lost due to product formation during a run, the Δmass is a negative value. We assume that this weight loss to largely due to the conversion of Si to gaseous product and hence associate $-\Delta$mass/h with the Si conversion rate.

shows that the rate of Si conversion (i.e., $-\Delta$mass/h) is 50% higher for the Sn-promoted sample than for the P-promoted sample. The MeCl conversion data, however, presented above show a value about 7 times higher for the Sn-promoted sample. We suspect that Cl deposition of the Sn-promoted contact mass is leading to a smaller difference in weight of the contact mass before and after MeCl exposure. We do not believe CH_3 groups (or fragments thereof) are responsible for the slight mass discrepancy in this case, since infrared data shown next suggest that coking or CH_3 fragmentation on the Sn-promoted contact mass is not occurring to a significant extent. However, even if the data in Fig. 4 are treated on a qualitative level, the observation that the Si conversion rate increases in the order of unpromoted < Zn-promoted < P-promoted < Sn-promoted agrees well with prior research [5].

It is useful to further compare our reaction results to those of prior studies of the action of promoters on the DS. The majority of prior research has been focused on the synergistic effects of multiply promoted contact masses [14]. Less research has investigated the reactivity and selectivity of singly promoted catalysts [11,15]. Prior research by Ward et al. showed that a Zn-promoted contact mass exhibited a higher TCMS/DMDCS ratio than a Sn-promoted contact mass (0.09 vs 0.12) [16]. The rate of product formation in the Sn-circumstance was over a factor of 2 greater than the Zn-promoted contact mass. Another prior study conducted by Rethwisch et al. showed a TCMS/DMDCS ratio of 0.34 for the Zn-promoted contact mass and a ratio of 0.58 for the Sn-promoted active mass [6]. On a qualitative level our results agree with these prior results. We find that Sn promotion results in the highest selectivity toward DMDCS, but it is only marginally higher than the selectivity exhibited for the Zn-promoted catalyst. Furthermore, we find that Sn promotion results in the highest MeCl and Si conversion rate. These experimental observations are consistent with the prior studies that show that Sn promotion increased the rate of methylchlorosilane production exceeding that of Zn promotion. We now present *in situ* infrared studies that help to develop a microscopic understanding of the origin of the different promoter actions.

3.2. In situ identification of surface intermediates on the DS contact masses

Fig. 5 displays *in situ* ATR-FTIR data associated with the CH stretching region that was obtained after the unpromoted, P-promoted, Zn-promoted, and Sn-promoted contact masses were exposed to argon for 3 h and then to MeCl for 0.5, 2, and 4 h at a temperature of 300 °C. Table 1 summarizes our mode assignments associated with the various surface species observed on the copper–silicon contact masses. All the spectra associated with MeCl exposure exhibit modes that are attributed to the C–H stretches of adsorbed CH_3 and fragment(s) of this group (i.e., $CH_{x=1,2}$). No evidence of gaseous MeCl modes was observed in any of the ATR-FTIR spectra.

We mention that all the plots include a spectrum labeled "under argon." This spectrum is representative of the respective contact mass after being exposed to a flow of Ar-gas for 3 h at 300 °C, prior to the introduction of MeCl. All these control spectra show minimal absorbance in the C–H region, emphasizing that absorbances that build up in this spectral region are due to the dissociative adsorption of MeCl on the contact mass surfaces.

Infrared modes that we attribute to adsorbed CH_3 are in good agreement with prior research that has investigated the thermal

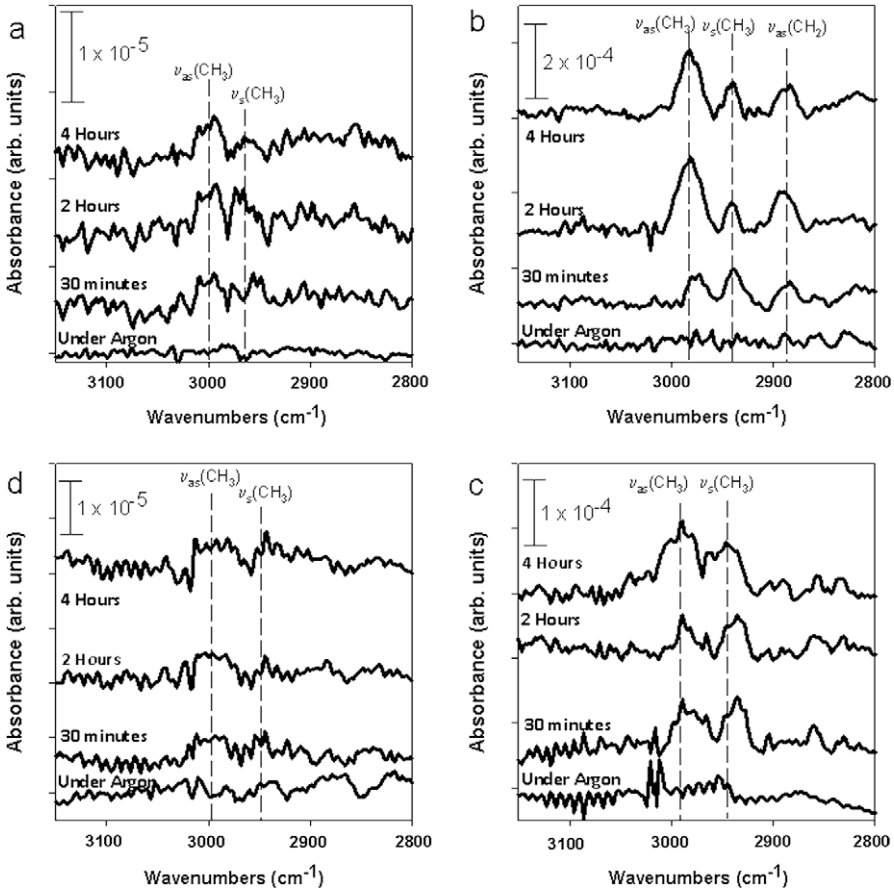

Fig. 5. ATR-FTIR of the CH stretching region for the (*clockwise from top left)* unpromoted (a), P-promoted (b), Sn-promoted (c), and Zn-promoted (d) contact masses as a function of reaction time at 1 bar MeCl at 300 °C. All the spectra were obtained *in situ*.

Table 1
Summary of assignments based on ATR-FTIR data (all data in cm^{-1}).

Surface species	Cu/Si	Zn/Cu/Si	P/Cu/Si	Sn/Cu/Si
$\nu_{as}(CH_3)$	3000	2995	2977	2988
$\nu_s(CH_3)$	2954	2950	2939	2940
$\nu_{as}(CH_2)$	–	–	2880	–
ν_{as}(Si–O–Si)	1193	1195	1190	1201
ν_s(Si–O–Si)	1051	1040	1030	1047
$\rho(CH_3)$	1276	1276	1276	1276
$\delta(CH_3)$[a]	~1205	~1205	~1205	~1205
ν_{as}(Si–O)	1120	1139	1122	1145
ν(C–O)[b]	–	–	–	1100
$\tau(CH_2)$	–	–	1010	–
ν_s(Si–O)	1004	990	980	990
$\delta(O_3Si–H)$	~900	~900	~900	~900
ν(Si–O)[b]	–	–	–	925
δ(Si–H)	~820	~820	~820	~820

[a] Obscured by ν_{as}(Si–O–Si) and is not labeled in figures.
[b] Resulting from methoxy absorbances.

chemistry of CH_3 on pure single crystalline silicon surfaces. Kong et al. investigated the thermal chemistry of CH_3 groups on Si(1 1 1) using infrared spectroscopy and assigned the asymmetric and symmetric methyl stretches to 2955 cm^{-1} and 2890 cm^{-1} absorption features, respectively [17]. In an earlier work, Colaianni et al. assigned the C–H stretches of CH_3 on silicon to absorbances at 2990 cm^{-1} and 2930 cm^{-1} [18]. Upon heating to 575 K they induced the fragmentation of the CH_3 group to an sp^3-hybridized CH_2 mode and assigned modes for this species at 2920 cm^{-1}, which is slightly higher than our assignment at 2880 cm^{-1} (most apparent on the P-promoted contact mass). The presence of promoter and/or copper on the surface of the contact mass provides likely explanations for the differences in C–H positions between this research and prior studies.

It is useful to bring forward some general observations that can be made concerning differences in the mode positions and relative mode intensities between the different contact mass formulations. After equivalent exposure times to MeCl at 300 °C, mode intensities attributable to CH_3 are higher by a factor of 10 (notice the absorbance scales) on the Sn-promoted and P-promoted contact masses than on the unpromoted and Zn-promoted contact masses. Associated with the P-promoted system, however, is an increase in mode intensity attributable to CH_2 that is greater than any other contact mass formulation.

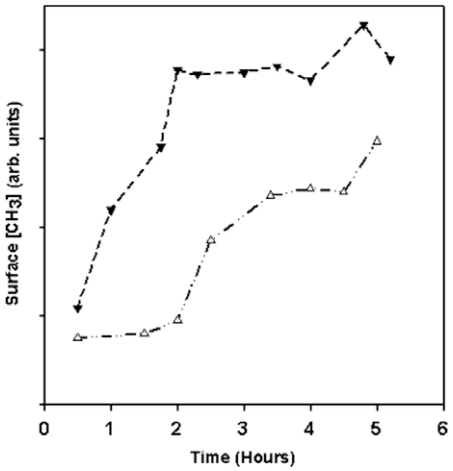

Fig. 6. Integrated peak areas for the asymmetric C–H stretching mode of CH_3 on the Sn- and P-promoted contact masses as a function of reaction time. The C–H stretching region associated with the Zn and unpromoted contact masses was too low to do a similar analysis.

Fig. 6 displays integrated peak areas of the $\nu_{as}(CH_3)$ mode for the Sn- and P-promoted contact masses over 5 h of reaction time. Note that integrated peak areas as a function of reaction time shown in Fig. 6 were derived from additional infrared data we obtained over what is displayed in Fig. 5. Our analysis was restricted to the Sn- and P-promoted surfaces due to the increased $\nu_{as}(CH_3)$ stretching intensity that allowed for more accurate peak fitting. Analyses of these data show that both surfaces exhibit a significant increase in CH_3 concentration over 5 h of reaction. After 2 h of reaction the surface CH_3 concentration associated with the P-promoted surface exceeds that of the Sn-promoted surface by a factor of ~2. While the P-promoted surface exhibits a relatively high CH_3 surface concentration, it does not exhibit a high MeCl conversion compared to the Sn-promoted contact mass. We infer from these experimental observations that the surface concentration of CH_3 alone is not a particularly good indicator of contact mass selectivity or reactivity. The low MeCl conversion associated with the P-promoted contact mass suggests that the CH_3 and surface hydrogen (from $CH_{x=1,2}$) that build up on this surface are not being converted to methylchlorosilane product as efficiently as on the Sn-promoted contact mass. In the Sn-promoted case, the MeCl conversion is as much as 7 times greater than that of the P-promoted surface. Based on this comparison, we speculate that the lower steady state CH_3 concentration on the Sn-promoted surface results from a more substantial fraction of the CH_3 resulting from MeCl dissociative chemisorption being converted to methylchlorosilane product than on the P-promoted surface. The increased fragmentation of the CH_3 group on the P-promoted surface is consistent with its selectivity toward DCMS, but this fragmentation may also be resulting in species (C, $CH_{x=1,2}$ and/or surface hydrogen) that bind to and block active Si sites that ultimately lead to the lower MeCl conversion. The slight decrease in MeCl conversion associated with the P-promoted surface (see Fig. 3) after 2–3 h of reaction may result from this coking of the surface.

The reason for the increase in MeCl conversion with time associated with the Sn-promoted surface is uncertain, but the result does suggest that the Sn-promoted contact mass is undergoing structural and/or compositional changes at the reacting surface during the DS reaction which are increasing its ability to form methylchlorosilane product. The Sn-promoted surface shows little evidence for the presence of C–H species that can be associated with CH_3 fragmentation, suggesting that this contact mass does not suffer from the coking and blocking of active sites that presumably is associated with the P-promoted surface. Hence, Sn promotion stabilizes the CH_3 group on the working surface.

Fig. 7 displays the 800–1300 cm^{-1} spectral range for the different contact masses for the same time sequence shown in Fig. 5 during their exposure to MeCl at 300 °C. Interestingly, the spectra are dominated by absorbances that we attribute to silicon–oxygen vibrations. Specifically, modes at 1190–1201 cm^{-1} and 1030–1051 cm^{-1} as well as modes at 1120–1145 cm^{-1} and 980–1004 cm^{-1} are assigned to silicon oxides and/or Si–O–Si suboxide networks. It is emphasized that these mode assignments are in excellent agreement with the extensive prior research that has investigated the oxidation of silicon surfaces [19].

We are not entirely certain why at least some oxide modes appear to increase in intensity with MeCl exposure time. We have carried out control experiments that exposed pure Si powder (no Cu or promoter) to Ar for 1 h and then to MeCl for 6 h. In this circumstance we see no change in the intensity of the silicon oxide modes associated with the silicon by infrared spectroscopy. Hence, we argue based on these experimental observations that the alloying reaction of Cu with Si at 300 °C is at the root of this phenomenon [20]. It seems likely that residual oxygen contamination in the gas stream oxidizes Si (in a copper silicide) during the reaction. It must be noted that copper silicide oxidizes extremely rapidly rel-

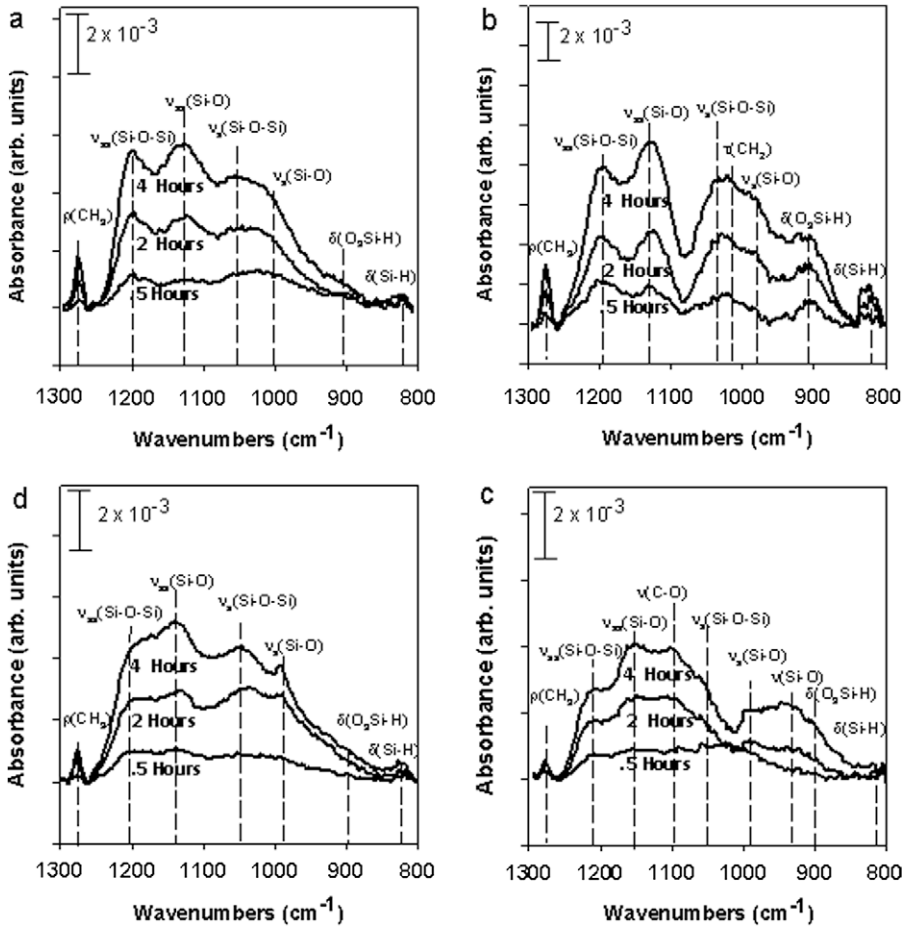

Fig. 7. The 800–1300 cm^{-1} spectral region for the (*clockwise from top left)* unpromoted (a), P-promoted (b), Sn-promoted (c), and Zn-promoted (d) contact masses after 0.5, 2, and 4 h of reaction time under MeCl at 300 °C. Mode assignments are listed in Table 1.

ative to silicon [21]. Interestingly, no prior *in situ* studies have probed the composition of the DS contact mass during the reaction. Hence, whether some oxidation of Si in the active Cu silicide component occurred in prior research or even in the working industrial catalyst cannot be addressed. We emphasize, however, that our reactor results are in good agreement with those of prior studies, and this brings up the possibility that oxygen impurities may play a role in altering the active site concentration (Si in the copper silicide) on the working DS catalyst.

Modes not associated with silicon oxides also appear in the 800–1300 cm^{-1} spectral region. One in particular that we attribute to a Si–H deformation mode, δ(Si–H), appears at 820 cm^{-1}. We believe a revealing aspect of these spectra is the increased absorbance due to Si–H in the case of the P-promoted contact mass and the absence of this absorbance in the Sn-promoted circumstance. This experimental observation is consistent with the P-promoted contact mass having a relatively high proportion of its C–H stretching intensity due to $CH_{x=1,2}$. Also, the absence of Si–H modes in the spectrum associated with the Sn-promoted mass is consistent with the lack of any significant $CH_{x=1,2}$ contribution to the C–H stretching region and is again consistent with the ability of Sn to stabilize CH_3 groups and prevent CH_3 decomposition on the contact mass surface.

Perhaps one of the more definitive peak assignments that can be made in the 800–1300 cm^{-1} spectral range is the $\rho(CH_3)$ mode at 1276 cm^{-1} that is due to CH_3 groups adsorbed on silicon [17,22]. We feel it is of note that the intensity of this peak does not vary dramatically between the different contact masses even though the Sn- and P-promoted contact masses exhibit C–H stretching spectral features at 2988 cm^{-1} and 2977 cm^{-1}, respectively, that are a factor of 10 greater than the unpromoted and Zn-promoted contact masses. At least a fraction of the C–H stretching intensity associated with the Sn-promoted contact mass could be due to the presence of surface methoxy (i.e., Si–OCH_3) group. This contention is bolstered by the appearance of a 1100-cm^{-1} mode that can be assigned to the ν(C–O) mode of methoxy in agreement with prior research of methoxy groups on Si single crystals [19]. The $\rho(CH_3)$ mode of methoxy typically appears near 1200 cm^{-1} [19], and this mode is presumably obscured by the relatively intense silicon oxide modes in this same region. A similar argument, however, cannot be made for the P-promoted contact mass (lacks an absorption feature at 1100 cm^{-1}), suggesting that the presence of methoxy cannot fully explain the lack of correspondence between the intensity of the $\nu(CH_3)$ and $\rho(CH_3)$ modes. It may be that the CH_3 coverage influences the $\nu(CH_3)$:$\rho(CH_3)$ ratio, but exploring this possibility will need to be addressed in further study.

While the presence of methoxy groups appears on the Sn-promoted contact mass surface, we cannot presume that these CH_3 groups leave the surface as methylchlorosilane product. We do suspect that this spillover of CH_3 groups to the silicon oxide is a result of the ability of the Sn-promoted contact mass to facilitate MeCl dissociative adsorption. The P-promoted contact mass also exhibits a mode near 900 cm^{-1}, which, based on prior research, is assigned to the $\delta(O_3Si–H)$ mode associated with hydrogen adsorbed on Si bound in a suboxide [19]. The presence of this mode is again consistent with the ability of the P-promoted contact mass

to dissociate surface CH_3. The P-promoted contact mass also exhibits a mode at 1010 cm^{-1} that can be attributed to a twisting mode of adsorbed CH_2, consistent with CH_3 fragmentation.

Interestingly, the Sn-promoted contact mass exhibits reduced spectral weight near 1060–1080 cm^{-1}, when compared to the unpromoted, P-promoted, and Zn-promoted contact masses at all the reaction times investigated with ATR-FTIR. Consistent with our contention above, we believe that the Si constituent of the Cu–Si alloy which forms in the contact mass undergoes a slow oxidation process with residual oxygen in the gaseous stream. We suggest that the presence of Sn inhibits Si oxide formation during or after the copper–silicon alloying reaction. This effect may be at least partly responsible for our experimental observation that the presence of Sn leads to a higher MeCl and Si conversion than the other contact masses.

While one of the promoter effects of Sn may be to stabilize the active copper silicide active site, another promoter action is to stabilize surface CH_3 and to prevent its dissociation to $CH_{x=1,2}$ species. Prior ultra-high vacuum-based research that investigated the effect of Sn on a single crystalline Si/Cu(100) surface supports this promoter effect of Sn [23]. In this prior study, the thermal chemistry of CH_3 on Si/Cu(100) led to the formation of trimethylsilane, but when Sn was present on the surface, tetramethylsilane was observed to desorb from the surface. This prior result again suggests that Sn inhibits the decomposition of surface CH_3 consistent with the Sn-promoted contact mass showing higher selectivity toward DMDCS. This effect of Sn directly contrasts the promoter action exhibited by P in this study. In the P circumstance, the conversion rate of Si is relatively high, but a significant amount of CH_3 dissociation is observed to occur on this surface which is likely responsible for its decreased selectivity for DMDCS and increased selectivity for the less methylated product DCMS.

3.3. General comments and some outstanding issues

Finally, we offer some general comments about Sn and Zn promotion based on our experimental results. First, while the selectivity toward DMDCS is slightly higher in the case of Sn promotion, the amount of product based on the MeCl and Si conversion data is at least a factor of 2 higher than when Zn is present. Second, our results are consistent with Sn carrying a higher CH_3 surface concentration than the Zn-promoted surface. The difference in CH_3 concentration between the two surfaces may be due to a higher rate of MeCl dissociative chemisorption on the Sn-promoted surface, relative to a Zn-promoted surface. Prior research has suggested that because of the low melting point of Sn (232 °C), this promoter may increase the DS rate at 300 °C by fluidizing the surface through a Sn-induced decrease in the surface [5]. It may be that the ability of Sn to spread on the working surface enables this element to exhibit its promoter effect over a significant portion of the active surface area of the contact mass. Based on our results these promoter effects likely include the stabilization of surface CH_3 and the prevention of the oxidative destruction of Si at active sites via its reaction with residual oxygen. Based on our experimental observations, the promoter action of Zn is different from that of Sn. In contrast to Sn-promoted contact mass, the Zn-promoted contact mass exhibits a surface CH_3 concentration during reaction that is closest to the unpromoted surface. The selectivity of the Zn-promoted surface toward DMDCS production and Si conversion rate, however, is significantly higher than the unpromoted contact mass even though the surface CH_3 concentration on both surfaces is similar. It may be that the promoter effect of Zn rests in its ability to increase the rate of active site formation (rather than affecting MeCl dissociative chemisorption), which has been suggested by prior research [8]. Such a possibility is presently being investigated in our laboratory by studying multiply promoted contact masses.

While we believe that the results of this study have given some insight into the effects of individual promoters on the DS, they have also brought up at least two issues that deserve further investigation. First, both the CH_3Cl conversion and CH_3 surface population increase over 6 h of the DS reaction under the experimental conditions used in the current study. Studies designed to investigate the changes on the contact mass during this period and to determine the point at which the CH_3 conversion achieves a constant value warrant attention in future studies. Second, the origin and effect of oxygen on the promoted DS contact masses also deserve further study. Our study suggests that Sn has an effect on Si–O bonds on the DS contact mass, but a more focused study on determining the effect of oxygen on the product selectivity also would appear to be a valid course of action in understanding the DS reaction.

4. Summary

The DS has been investigated on Zn-promoted, Sn-promoted, P-promoted, and unpromoted copper–silicon contact masses at 1 bar MeCl at 300 °C. The Sn-promoted contact mass exhibits the highest reactivity as measured by its Si conversion rate and selectivity toward DMDCS. *In situ* ATR-FTIR shows that this catalyst has a relatively high surface concentration of CH_3, but it is lower than that associated with the P-promoted catalyst. P-promotion increases the rate of Si conversion relative to both the Zn-promoted and unpromoted contact masses, but this promoter leads to the dissociation of surface CH_3 that goes on to form $CH_{x=1,2}$ surface species. Also, this contact mass formulation is most selective toward DCMS. At least a fraction of the methyl that is observable with ATR-FTIR on the Sn-promoted contact mass is thought to be due to methoxy groups that form on residual oxide associated with the Si component. The steady state concentration of CH_3 on the Zn-promoted catalyst was significantly less than either the Sn- or P-promoted contact masses, and was similar to the unpromoted sample. However, the Zn-promoted contact mass showed a high selectivity toward DMDCS.

Acknowledgment

D.R.S. and B.J.H. greatly appreciate financial support from the National Science Foundation (Grant #CHE0517017).

References

[1] E.G. Rochow, Journal of the American Chemical Society 67 (1945) 963–965.
[2] D. Seyferth, Organometallics 20 (2001) 4978–4992.
[3] K.M. Lewis, B. Kanner, Catalyzed Direct Reactions of Silicon, Elsevier, Amsterdam, 1993.
[4] L.N. Lewis, Chemistry of Organic Silicon Compounds 2 (1998) 1581–1597.
[5] R.J.H. Voorhoeve, Organohalosilanes: Precursors of Silicones, Elsevier, Amsterdam, 1967.
[6] L.D. Gasper-Galvin, D.M. Sevenich, H.B. Friedrich, D.G. Rethwisch, Journal of Catalysis 128 (1991) 468–478.
[7] L.D. Gasper-Galvin, D.G. Rethwisch, D.M. Sevenich, H.B. Friedrich, Studies in Organic Chemistry (Amsterdam) 49 (1993) 279–297.
[8] N. Floquet, S. Yilmaz, J.L. Falconer, Journal of Catalysis 148 (1994) 348–368.
[9] R.L. Halm, R.H. Zapp, R.D. Streu, Reduced formation of methyltrichlorosilane in the Rochow process in the presence of hydrogen, US Patent Number 4,762,940, Dow Corning Corp., USA, 1990.
[10] D.G. Rethwisch, J.F. Olakangil, L.H. Wood, D.C. Miller, J.D. Wineland, in: Silicon for the Chemical Industry VI, Conference, Loen, Norway, June 17–21, 2002, pp. 313–321.
[11] H. Ehrich, D. Born, K. Richter, J. Richter-Mendau, H. Lieske, Applied Organometallic Chemistry 11 (1997) 237–247.
[12] H. Lieske, H. Fichtner, I. Grohmann, M. Selenina, W. Walkow, R. Zimmermann, in: Silicon Chem. Ind. Int. Conf., 1992, pp. 111–118.
[13] H. Ehrich, D. Born, J. Richter-Mendau, H. Lieske, Applied Organometallic Chemistry 12 (1998) 257–264.

[14] T.J. Wessel, D.G. Rethwisch, Reaction Kinetics and Catalysis Letters 58 (1996) 7–12.
[15] J.P. Agarwala, J.L. Falconer, International Journal of Chemical Kinetics 19 (1987) 519–537.
[16] W.J. Ward, A. Ritzer, K.M. Carroll, J.W. Flock, Journal of Catalysis 100 (1986) 240–249.
[17] Maynard J. Kong, Julia Lyubovitsky, Stacey F. Bent, Chemical Physics Letters 263 (1996) 1–7.
[18] M.L. Colaianni, P.J. Chen, H. Gutleben, J.T. Yates Jr., Chemical Physics Letters 191 (1992) 561–568.
[19] D.J. Michalak, S.R. Amy, A. Esteve, Y.J. Chabal, Journal of Physical Chemistry C 112 (2008) 11907–11919.
[20] R.J.H. Voorhoeve, J.A. Lips, J.C. Vlugter, Journal of Catalysis 3 (1964) 414–425.
[21] S.H. Corn, J.L. Falconer, A.W. Czanderna, Journal of Vacuum Science and Technology A 6 (1988) 1012–1016.
[22] J.A. Glass Jr., E.A. Wovchko, J.T. Yates Jr., Surface Science 338 (1995) 125–137.
[23] X.V. Zhang, D.R. Strongin, L.V. Goncharova, A.V. Ermakov, B.J. Hinch, Journal of Physical Chemistry B 108 (2004) 16213–16219.